# A new angle on contour integration: The role of corners

## Malte Persike

Psychological Institute, Johannes Gutenberg University, Mainz, Germany

## Günter Meinhardt

Psychological Institute, Johannes Gutenberg University, Mainz, Germany

**Contour integration refers to the binding of disjoint local segments into contiguous global shapes. One central tenet in the study of contour integration has been the dependency of contour visibility on curvature. When contours become increasingly jagged, contour salience deteriorates down to the point of invisibility. In this study, we show that the deterioration of contour visibility due to sharp changes in curvature can be easily remedied by inserting corner elements at the points of angular discontinuity. Corners render even highly bent contours as salient as straight ones. We find contour integration with corners to be psychophysically indistinguishable from the integration of perfectly straight contours. Corners thereby enable a more general form of good continuation, which no longer relies on smooth curvature but merely on the presence of sufficiently predictive signals of direction and directional change. This challenges established theories of human contour integration that rely on local interactions between orientation sensitive neurons early in the visual pathway, the so-called *association field* models. The capacity to seamlessly integrate orientation signals with vastly different complexities, such as straight lines and corners, likely places contour completion with other image composition mechanisms beyond primary visual cortex.**

## Introduction

The fragmentation of object outlines into assemblies of discrete local segments is one of the major challenges for visual scene processing (Wagemans et al., 2012). One familiar example is the rooftop behind trees, where a contiguous edge is turned into an array of perceptually disconnected local elements. Contour integration is the process of binding such elements into a whole percept (Field, Hayes, & Hess, 1993). It can operate on many different element properties such as coherent motion (Ledgeway, Hess, & Geisler, 2005), a common temporal frequency (Alais, Blake, & Lee, 1998), or a continuous plane of depth (Hess, Hayes, & Kingdom, 1997). The most scrutinized variant of contour integration, however, is the linking of local elements based on orientation collinearity (Hess & Field, 1999). It requires contour elements to fall on a smooth spatial global trajectory and their orientations to coalign with said trajectory (Hess & Dakin, 1997). Contour visibility deteriorates if bends along the trajectory become too sharp (Pettet, 1999) or local element orientations deviate too much from global curvature (Ledgeway et al., 2005).

This notion has shaped our current understanding of contour integration. The *association field* has been popularized as a highly influential model explaining the integration of noncontinuous visual contours from predominantly local processes, based on the mutual facilitation of neighboring orientation selective neurons with similar orientation tuning (Field et al., 1993). The association field model is preceded by a similar theory that proposes a boundary completion mechanism sensitive to collinear orientations of local elements across perceptual space (Grossberg & Mingolla, 1985a, 1985b). A large number of psychophysical studies and electrophysiological investigations have corroborated the underlying idea that horizontal projections among orientation detectors early in the visual pathway may serve as the neural substrate of the association field (Hess & Field, 1999). Intercolumnar synaptic fibers spanning preferentially between neurons with similar orientation tuning have indeed been found in the visual cortex of monkeys (Stettler, Das, Bennett, & Gilbert, 2002) and cats (Kinoshita, Gilbert, & Das, 2009), although the correspondence between spatial dynamics of contour integration and the characteristics of horizontal connections is far from definitive (Angelucci et al., 2002).

One of the hallmarks of contour integration is its susceptibility against curvature. All association field models reflect this property by letting the binding strength between neighboring elements be a function of their orientation similarity (Ernst et al., 2012; Li, 1998;

Mundhenk & Itti, 2005). Whenever adjacent contour elements assume increasingly different orientations, global contour saliency deteriorates down to the point of invisibility. This notion has garnered overwhelming empirical support (Hess & Field, 1999), yet it is dependent on one important precursor: local elements are assumed to carry only one orientation component. Each individual contour element is *mono-oriented* in the sense of a straight line. This presents a severe empirical restriction given that research has emphasized the important role of corners and junctions for the processing of object shape (Biederman, 1987; Marr, 1980). Corners contribute more to shape processing than straight edges (Poirier & Wilson, 2007), possibly because they serve as salient cues for local image complexity (Heitger, Rosenthaler, von der Heydt, Peterhans, & Kubler, 1992; Rodrigues & du Buf, 2006). From an information theory perspective, corners carry high informational value for global shape analysis (Attneave, 1954; Feldman & Singh, 2005), which is expressed by the fact that at locations of angular discontinuity, an observer can no longer predict the continuation of an object outline reliably from its previous course (Shevelev, Kamenkovich, & Sharaev, 2003).

Stimuli used in contour integration research are devoid of visible corner elements. Contours are usually assembled from collinear broadband or band-pass elements with only one single orientation component, embedded in larger ensembles of similar elements with random orientation (Dakin & Hess, 1999). The notion of a corner (Bowden, Dickinson, Fox, & Badcock, 2015), turning point (Mathes & Fahle, 2007), or acute angle (Geisler, Perry, Super, & Gallogly, 2001) in contour integration thus always describes directional changes along the projected trajectory of a contour, but never the geometry of its visible local elements. Sharp changes in curvature along such contours necessarily impose vastly different orientations on the elements adjacent to the point of angular discontinuity, which has proven detrimental to contour visibility (Field et al., 1993; Pettet, 1999). Research on contour integration as one of the fundamental mechanisms of perceptual completion (Wagemans et al., 2012) has hitherto sidestepped the role of corners or any other type of nonlinear local element for scene composition. This is striking not only from an experimental perspective but has also left its mark on computational approaches to contour integration. With very few exceptions (Parent & Zucker, 1989), computational models have been developed with a strict focus on mono-oriented local elements (Choe & Miikkulainen, 2004; Ernst et al., 2012; Li, 1998; Ursino & La Cara, 2004; Williams & Thornber, 2001; Yen & Finkel, 1998).

The visual system is well equipped for processing corners even at early stages along the visual hierarchy.

Already in primary visual cortex, the outputs from endstopped cells can account for the percept of a corner (Rodrigues & du Buf, 2006), albeit not by means of individual neurons but through a network of multiple detector units (Roelfsema, Lamme, Spekreijse, & Bosch, 2002). Single neurons selective for stimulus characteristics like the sign of curvature, the polarity of angles, or the angular value itself have been reported no earlier than V2 (Ito & Komatsu, 2004). A considerable portion of orientation selective V2 neurons exhibit a bimodal response profile tuned to two different orientations within the same receptive field (Anzai, Peng, & Van Essen, 2007). Although bimodal specifity is a necessary condition for corner detection, these V2 neurons are still unfit for corner detection since their responses to the optimal angle is indistinguishable from the response to either orientation component (Ito & Komatsu, 2004). Specialized corner detectors finally emerge in area V4, where many cells respond preferentially to corners and curves but not the constituting orientations in isolation (Pasupathy & Connor, 2002). Given that recent studies have also proposed area V4 as one of the main loci of contour integration (Chen et al., 2014; Gilad, Meirovithz, & Slovin, 2013), it stands to reason that contour detection may benefit from the presence of corner elements along a contour.

In the present study, we first examine the role of corner elements in contour integration and try to narrow down the geometric properties that define an effective corner. Moreover, we investigate the spatial and temporal dynamics of contour integration with and without corners in order to discern whether a common neural process may be responsible for both. We finally assess whether contour integration is functional for contour stimuli that satisfy the collinearity principle but contain nothing but corners.

## Methods

### Stimuli

Stimuli in Experiments 1, 2, and 3 were constructed from either Gabor elements or line elements. Gabors were defined by

$$g(x,y) = \exp\left(-\frac{x^2 + y^2}{2\sigma^2}\right)$$
$$\times \sin\left(2\pi f\left(x\cos\left(\frac{\varphi}{180}\pi\right) - y\sin\left(\frac{\varphi}{180}\pi\right)\right)\right). \quad (1)$$

Carrier spatial frequency was fixed at $f = 3.25$ cycles per degree of visual angle. Gabors had a standard deviation of $\sigma = 0.24°$ visual angle and were clipped beyond a radius of 2.75 $\sigma$-units. Spatial phase alternated
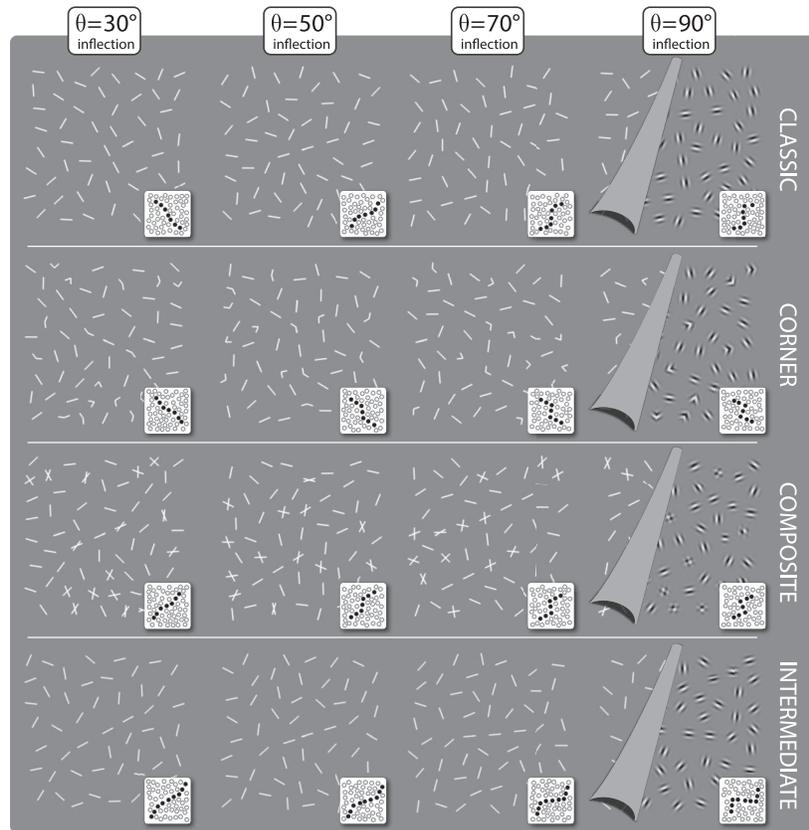
Figure 1. Stimulus illustrations from Experiment 1. Shown are examples of all contour configurations for inflection angles of 30°, 50°, 70°, and 90°. The 0° inflection angle is not included since it always produces a perfectly straight contour. Stimulus examples are mostly constructed from line elements, illustrations of Gabor stimuli are shown as inserts. Contours always had two points of angular discontinuity with opposite sign but constant angle. To equate the composition of contour and background in the respective conditions, corners or crossings were inserted into the background at approximately the same ratio as along the contour. Angles of background corners and crossings were sampled randomly from the predefined set of possible angles. Note that only the inner 10° × 10° region of the whole 17° × 17° stimulus is shown.

randomly between phase and counterphase sines. Gabor elements induce a band-pass response from visual filters at early stages of the visual hierarchy. The composition of a corner from two halves of a Gabor element brings significant changes to the spatial frequency spectrum when compared with a mono-oriented Gabor. Broadband elements such as thin lines mitigate the difference in frequency response between corners and mono-oriented elements. The spatial frequency spectra of an angled line and of an ensemble of two unconnected straight lines with the same angular difference are considerably more similar than in the Gabor case, which is why we decided to duplicate each experiment and use line elements as a second stimulus variant. Line elements had a length of 1.1° visual angle, a line thickness of 4 pixels, and were smoothened by a Gaussian kernel with a standard deviation of 0.75 pixels.

In addition to these mono-oriented elements, we defined corner elements carrying two orientation components. Orientations within each element differed by an angle $\pm\theta'$, hence components touched along a boundary of $\pm0.5\theta'$ relative to the orientation of each component (see Figure 1). Further, we defined crossings as a simple superposition of two elements with different orientations.

Experiments 4 and 5 further contained Gaussian blobs or simple discs. Gaussian blobs were defined as

$$b(x, y) = \exp\left(-\frac{x^2 + y^2}{2\sigma^2}\right). \quad (2)$$

Discs had a diameter of 0.3° visual angle and were smoothened by a Gaussian kernel with a standard deviation of 0.75 pixels.

The general stimulus creation process was identical for all experiments. After a contour was created and elements placed along its trajectory, the contour was superimposed onto a hexagonal grid of 203 background elements. The center of a contour was always

placed within the central $10° \times 10°$ region of the whole $17° \times 17°$ stimulus area to prevent contours from extending too far into the peripheral field where contour integration is known to be absent (Hess & Dakin, 1997). Background elements overlapped by the contour were removed from the grid. Finally, background elements were displaced using a stochastic diffusion algorithm (Ernst et al., 2012). Euclidian distances between adjacent contour elements were also randomized according to the natural neighbor distribution of background elements, as determined in prior simulations, and had a mean of about $1.34°$. Orientations of background elements were sampled uniformly from the interval $[0° \ldots 360°]$, as were the orientations of contour elements in distracter stimuli. Orientation components of contour elements in target stimuli were always perfectly collinear with the global trajectory. In conditions where corners or crossings were embedded along the contour trajectory, the same element type was placed into the background at approximately the same ratio as along the contour. Hence, neither the presence nor the spatial density of corners or crossings was indicative of a target stimulus.

## Sample

All experiments were completed by 20 observers (age range 18 to 29 years; 14 women, six men), a small subset of which took part in more than one of the experiments. Participants received course credits or were paid upon completing the experiments. All observers had normal or corrected to normal vision.

## Ethics statement

Prior to the experiment, participants were informed about the course and expected duration of the experiment. They received a general description of the purpose of the experiment but not about specific outcome expectations. All participants signed a written consent form according to the World Medical Association Helsinki Declaration and were informed that they could withdraw from the experiment at any time without penalty. Noninvasive experimental studies without deception do not require a formal review by the institutional ethics committee, provided the experiment complies with the relevant regulations and legislation, which was carefully ascertained by the authors. After completing the experiment, a summary of their individual data was shown to the observers and the results pattern explained.

## Task

All experiments used a temporal two-alternative forced choice (2AFC) contour detection task. After the initial fixation marker (500 ms) participants saw the first stimulus screen, followed by a noise mask (500 ms). The whole sequence was repeated for the second stimulus screen. Each trial terminated with a blank screen until response. Unless stated otherwise, presentation time for both stimulus screens was fixed at 350 ms. Participants indicated with a button press which of the two stimulus screens contained the contour. The experiment started with a training period using highly salient target stimuli to practice response key assignment until at least 93.75% correct responses were achieved. During training and the subsequent main experiment, each condition was executed with 32 replications.

## Apparatus

Stimuli were generated on a ViSaGe graphics adapter (Cambridge Research Systems, Rochester, UK) and displayed on a Samsung 959NF color monitor. The mean luminance of the screen was 51.1 cd/m$^2$. Stimuli were displayed with a fixed Michelson contrast of 0.964. Gray values were taken from a gamma-corrected linear staircase consisting of 255 steps. Linearity was checked with a ColorCAL colorimeter (Cambridge Research Systems). The refresh rate of the monitor was 75 Hz, the pixel resolution was set to $1280 \times 1024$ pixels. The room was darkened so that the ambient illumination approximately matched the illumination of the screen. Stimuli were viewed binocularly at a distance of 70 cm. Participants used a chin rest for head stabilization and gave responses with their dominant hand via an external keypad.

## Performance measures

Data analysis in a factorial design requires an unbounded variable at interval measurement level. Proportion correct is not appropriate since it is a bounded measure whose distribution becomes severely skewed as the mean approaches either bound of the scale. The sensitivity measure $d'$ avoids this disadvantage. In a 2AFC task, $d'$ is obtained from proportion correct by $d' = \sqrt{2}\Phi^{-1}(p)$. Proportions correct for perfect performance were replaced by $1 - (2n)^{-1}$, where $n$ is the number of replications. All data plots depicted here show proportion correct as well as $d'$ values. Statistical analyses were conducted on $d'$ values.

Sensitivity data were analyzed by repeated measures analysis of variance (rmANOVA) at $\alpha = .01$.

## Experiment 1: Contour integration with corners

### Methods and design

Contours in Experiment 1 were composed from three straight backbone segments, connecting at angles of $\theta = \pm[0°, 30°, 50°, 70°, \text{or } 90°]$. A nonzero value of $\theta$ creates two points of angular discontinuity between segments. The principal direction of each contour was sampled randomly from $[0° \ldots 360°]$.

Contours were displayed in one of four configurations (Figure 1). First, the CLASSIC configuration represented the stimulus type commonly used in contour integration research. All contour elements exhibited a single orientation component collinear with the global trajectory. Points of angular discontinuity always fell between two neighboring contour elements. Second, in the CORNER configuration, corner elements were placed at the points of angular disparity. The orientation components of each corner element were always collinear with the connecting path segments. Third, the COMPOSITE configuration focused on the fact that corner detection in the human visual system has different levels of refinement. Shapes like + and ⊥ may evoke identical responses from accordingly tuned V2 cells but no longer from cells in V4 (Ito & Komatsu, 2004; Pasupathy & Connor, 2002). This raises the question as to what qualifies as a corner in contour integration. To mark out the geometric properties of effective corner elements, the COMPOSITE configuration therefore placed crossings instead of corners at locations of angular discontinuity. Contours in the aforementioned three configurations always comprised seven Gabor or line elements. Fourth, the INTERMEDIATE configuration addressed possible confounds associated with the introduction of corner elements. The first confound is contour length. Research has shown that longer contours enjoy a saliency advantage (Vancleef & Wagemans, 2013). A corner elicits two separate orientation signals at its spatial location that could be considered to increase the quantity of distinct orientation components along a contour, thus enhancing contour visibility. The second confound relates to the perceived angle of corner elements. If the visual system simply averaged over the two orientation components of a corner element, corners would act as intermediate elements that reduce the angular disparity between adjacent path segments, again possibly enhancing contour visibility. The INTERMEDIATE condition therefore extends the CLASSIC configuration by
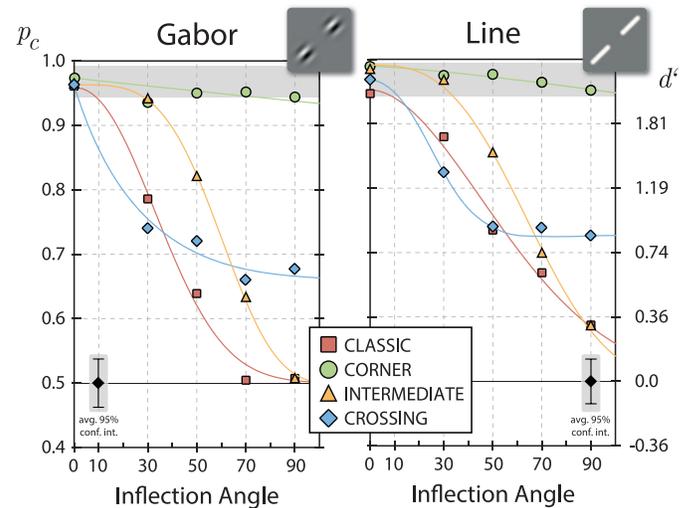


Figure 2. Results from Experiment 1. Graphs depict detection performance for the different contour configurations across increasing levels of angular discontinuity, split by local element type. Colored dots represent mean performance across all participants. The secondary axis depicts $d'$ values corresponding to the proportion correct scale. The shaded area at the top of each graph is the 95% confidence region derived from the detection rates of perfectly straight contours. To facilitate legibility of the individual plots, the average 95% confidence interval for the mean across all conditions is given.

inserting mono-oriented elements at the points of discontinuity. These elements had an orientation midway between the orientations of the two connecting path segments, hence attenuating the orientation disparity between two adjacent path segments and also increasing path length to nine elements.

Contour integration performance for the four different contour configurations was probed at five inflection angles ranging from 0° to 90°. Element type and contour configuration were run in blocks, corner angles were randomly interleaved within each block. Sensitivity data from $n = 20$ observers (16 women, four men) were analyzed separately for Gabor and line stimuli by repeated measures analysis of variance (rmANOVA) with contour configuration and corner angle as factors.

### Results

The pattern of results is similar for Gabor and line elements (Figure 2). We find a main effect for contour configuration with both Gabor, $F = 111.6$; $df = 3, 57$; $p < 0.001$, and line elements, $F = 97.1$; $df = 3, 57$; $p < 0.001$. Detection performance is highest for contours with corner elements, followed by contours with intermediate mono-oriented elements and crossings at the points of discontinuity, and lowest for classic

contours. We observe a second main effect for inflection angle with both Gabor, $F = 153.7$; $df = 4, 76$; $p < 0.001$, and line elements, $F = 214.5$; $df = 4, 76$; $p < 0.00$, indicating that performance declines with increasing inflection angle. This, however, does not apply to all contour configurations, as indicated by a significant interaction between configuration and inflection angle for Gabor, $F = 32.8$; $df = 12, 228$; $p < 0.001$, and line contours, $F = 25.8$; $df = 12, 228$; $p < 0.001$. We observe that the visibility of even highly bent contours can remain on par with straight contours if and only if corner elements are inserted at the points of angular discontinuity. For all other contour configurations, contour detection performance deteriorates with increasing angular discontinuity. It should be noted that the decline for crossings is somewhat different from what was observed for mono-oriented elements. Contour integration performance with crossings also declines at first but stabilizes at about 70% correct responses for larger inflection angles instead of falling entirely to chance level.

Results suggest that only elements with the specific geometric properties of corners are able to effectively connect contour segments across angular discontinuities. Does the perception of contours with and without corner elements invoke the same neural mechanisms? One way to approach this question is to take well-known characteristics of human contour integration and demonstrate psychophysical equivalence of contours with and without corners.

# Experiment 2: Temporal dynamics

## Methods and design

Experiment 2 investigated the temporal dynamics of contour integration with and without corner elements. Contour integration is known to benefit from longer inspection times. While monkeys achieve near perfect contour detection performance already at brief stimulus durations of 30–60 ms (Mandon & Kreiter, 2005), human contour integration takes around 200–300 ms to saturate (Braun, 1999). More rapid contour integration in humans has been observed only for longer contours with at least 10 elements (Vancleef & Wagemans, 2013).

To assess the time course of contour integration with corners, we presented contours identical to the CORNER configuration from the first experiment with five inflection angles ranging from 0° to 90° and let inspection times vary from 50, 100, 150, 250, to 350 ms. Element type was run in blocks, inspection times and corner angles were randomly interleaved within each block. Sensitivity data from $n = 20$ observers (15 women, five men) were analyzed separately for Gabor
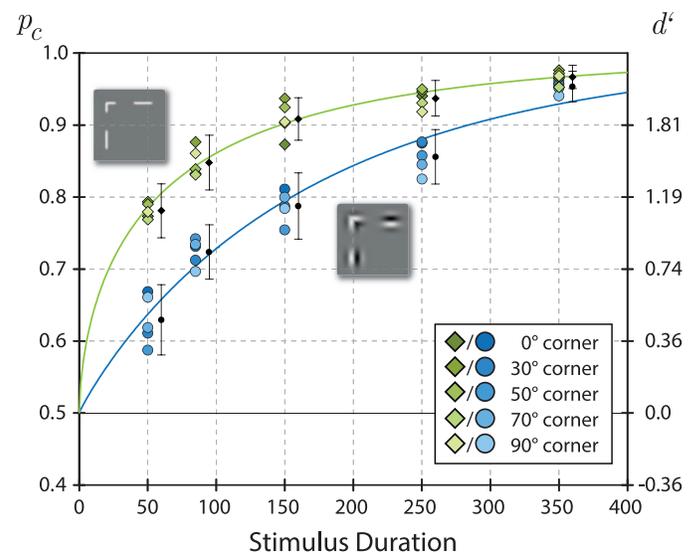


Figure 3. Results from Experiment 2. Shown are detection performances for contours with different corner angles over increasing inspection times. Colored dots represent the mean detection performance across all participants for contours constructed from line elements (green) or Gabors (blue). Error bars illustrate the 95% confidence limit for the mean, derived from 0° (i.e., straight) contours only.

and line stimuli by rmANOVA with inspection time and corner angle as factors.

## Results

The pattern of results is similar for Gabor and line contours (Figure 3), aside from an overall higher level of performance for line elements. We find a main effect of presentation time on the visibility of contours with both Gabor, $F = 231.508$; $df = 4, 76$; $p < 0.001$, and line elements, $F = 124.924$; $df = 4, 76$; $p < 0.001$. Detection performance increases as inspection times become more relaxed. The course of increase is practically identical from straight contours to the highest corner angle. This is confirmed by the absence of a main effect for inflection angle, as well as a nonsignificant interaction between presentation time and inflection angle (both $p > 0.05$).

The contour integration process evidently follows similar time courses for perfectly straight contours and contours with corner elements. Not only are the temporal dynamics practically identical across different degrees of angular discontinuity, they also correspond well with earlier research, where contours were barely visible for brief exposure durations of 30 ms and performance reached a plateau around 300 ms (Braun, 1999). Moreover, the observed general detectability advantage for contours with phase-aligned broadband elements such as edges or lines has also been reported before (Dakin & Hess, 1999).
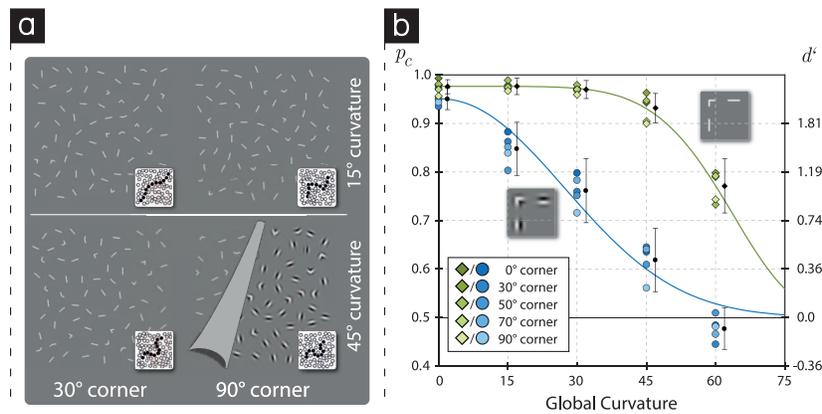
Figure 4. Stimulus illustrations and results from Experiment 3. (a) Exemplary combinations of global curvature and corner angle. Stimulus examples depict line elements, an instance of a Gabor stimulus is shown in the lower right. (b) Detection performance for contours with different corner angles across increasing levels of curvature. Colored dots represent the mean detection performance across all participants for line elements (green) and Gabors (blue). Error bars illustrate the 95% confidence limit for the mean, derived from 0° (i.e., straight) contours only. Note that only the inner 10° × 10° region of the whole 17° × 17° stimulus is shown.

# Experiment 3: Curvature

## Methods and design

One of the defining features of human contour integration is the deterioration of detection performance with increasing curvature (Field et al., 1993; Pettet, 1999). If the same neural mechanisms govern the integration of contours with and without corners, the course of visibility reduction due to increments in contour curvature should be similar. Experiment 3 therefore studied the impact of global curvature on contour integration performance with different corner angles. We presented contours similar to the corner configuration from the first experiment and had the orientation of each contour element deviate from its neighbors by levels of $\Delta_\varphi = \pm[15°, 30°, 45°, 60°]$, thus creating a global curvature of constant radius (Figure 4a). To create a pronounced depiction of curvature, contours comprised 12 elements.

Contour integration performance for the different curvatures was measured for five inflection angles ranging from 0° to 90°. Element type was run in blocks, curvature angles and corner angles were randomly interleaved within each block. Sensitivity data from $n = 20$ observers (17 women, three men) were analyzed separately for Gabor and line stimuli by rmANOVA with curvature and corner angle as factors.

## Results

The pattern of results is similar for both types of elements (Figure 4b), again with a general sensitivity advantage for contours with line elements. Results show a main effect of global curvature for both Gabor, $F = 114.912$; $df = 3, 57$; $p < 0.001$, and line based contours, $F = 158.848$; $df = 3, 57$; $p < 0.001$. Contour visibility decreases as the inter-element angles between adjacent contour elements become more disparate. This effect of contour curvature on contour integration is independent of corner angle, indicated by an insignificant interaction between curvature level and corner angle, as well as the absence of an overall effect of corner angle (both $p > 0.05$). The function of visibility decrease with increasing curvature is practically identical between contours with arbitrary corner angles and perfectly straight contours.

We take this as evidence that the major determinant for the salience of curved contours is the angular mismatch between neighboring contour elements, regardless of whether these elements are mono-oriented or corners. Corner elements integrate seamlessly with mono-oriented elements during contour formation. For Gabor elements, results comply with the existing literature, in which detection performance halved for a global curvature of 30° and dropped to chance at about 60° (Field et al., 1993; Hess & Field, 1999).

# Experiments 4 and 5: Elimination of mono-oriented elements

## Methods and design

Stimulus configurations in the previous experiments always intermixed corners with mono-oriented elements. This permits an alternative interpretation of our results where contour integration is not the primary mechanism of target detection. Corners are known to
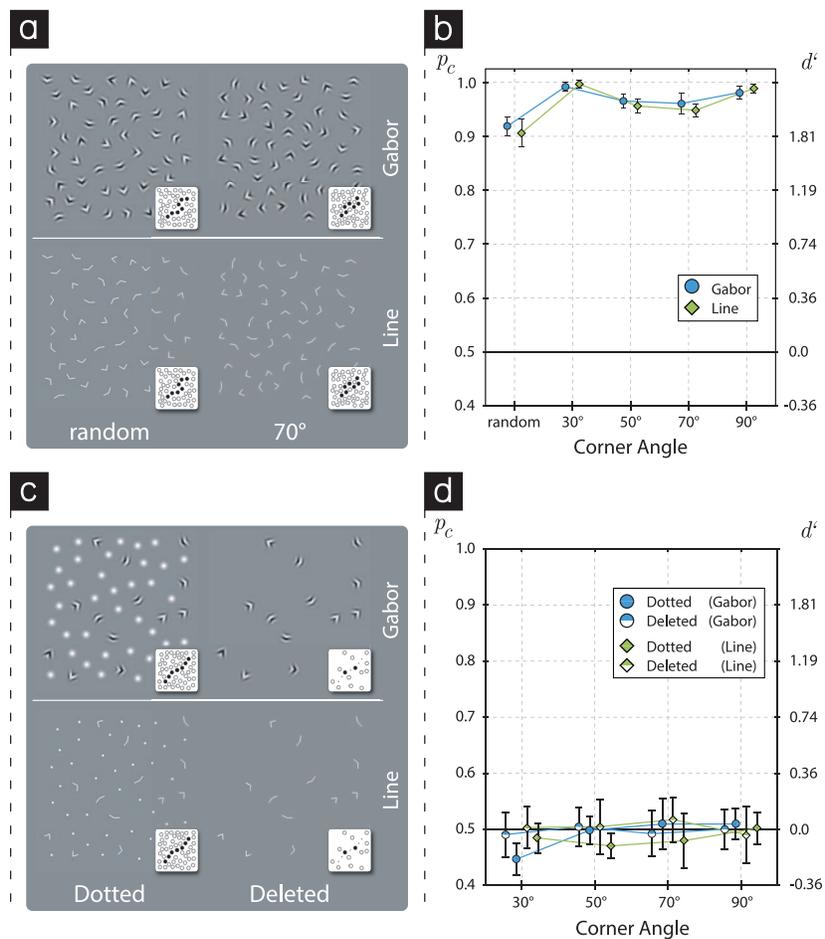
Figure 5. Stimulus illustrations and results from Experiments 4 and 5. (a) Exemplary "all-corner" contours from Experiment 4, shown for two angle variants: random corner angles and a fixed corner angle of 70°. (b) Detection performance for contours across five corner angle conditions in Experiment 4. (c) Exemplary contours from Experiment 5, each at a 30° corner angle. (d) Detection performance for contours across four corner angles in Experiment 5. All stimulus examples are depicted in both Gabor and line variants. Colored dots always represent the mean detection performance across all participants for line elements (green) and Gabors (blue). Error bars illustrate the 95% confidence limit for the mean. Note that only the inner 10° × 10° region of the whole 17° × 17° stimulus is shown.

be potent attractors of involuntary visual-spatial attention (Burnham & Neely, 2007), leading to enhanced processing of image regions in the vicinity of corners—the "corner enhancement effect" (Cole, Skarratt, & Gellatly, 2007). Targets presented spatially close to a corner are detected more efficiently than targets presented near straight edges (Cole, Gellatly, & Blurton, 2001), particularly when the corner is part of an object (Bertamini, Helmy, & Bates, 2013). If one assumes that target detection in our experiments was achieved by the visual system merely scanning the vicinity of corner elements for mono-oriented elements with matching orientations, the corner enhancement effect might have contributed significantly to the high saliency of contours.

A straightforward way to examine this idea is to generate stimuli without mono-oriented elements. We took two avenues of approach. In Experiment 4, we

created stimuli comprising nothing but corner elements (Figure 5a), which we shall call "all-corner" stimuli. Contours were assemblies of seven corner elements whose orientation components were always collinear with the respective leg of the neighboring corners. The angles of corner elements were either sampled randomly from $\theta = \pm[30°, 50°, 70°, 90°]$, or were fixed at one angle thereof. The angular direction of each contour corner was chosen in a pseudo-random procedure ensuring that a contour would not intersect itself. The angles of corner elements in the background were always sampled randomly from the set of possible corner angles. Contour integration performance was measured for the five angle conditions [random, 30°, 50°, 70°, 90°]. Element type was run in blocks, corner angle was randomly interleaved within each block. Sensitivity data from $n = 20$ observers (15 women, five men) were analyzed

separately for Gabor and line stimuli by rmANOVA with corner angle as the factor.

In Experiment 5, we used stimuli identical to the CORNER configuration from Experiment 1 and either deleted all straight elements or replaced them with unoriented elements (Figure 5c). Contour integration performance for the two deletion conditions was measured for the four inflection angles [30°, 50°, 70°, 90°]. Element type was run in blocks, corner angle was randomly interleaved within each block. Sensitivity data from $n = 20$ observers (15 women, five men) were analyzed separately for Gabor and line stimuli by rmANOVA with corner angle as the factor.

## Results

The pattern of results in Experiment 4 is highly similar for Gabor and line contours (Figure 5). Although corner angle has a significant effect on contour visibility with both Gabor, $F = 15.231$; $df = 4, 76$; $p < 0.001$; $\eta^2 = .445$, and line elements, $F = 26.304$; $df = 4, 76$; $p < 0.001$; $\eta^2 = .581$, the effect is small in absolute terms. Contour detection performance with all-corner stimuli remains above 90% correct for all angle variants. Contours with homogenous corner angles even retain performance levels of at least 94.8%.

A markedly different picture emerges when mono-oriented elements are deleted from a stimulus or replaced by non-oriented dots in Experiment 5. Corner elements, even if perfectly aligned, are neither integrated across larger distances nor do they enable observers to connect intermediate segments of dotted lines. Detection performance remains at chance level and no main or interaction effects reach significance in any of the conditions (all $p \geq 0.151$).

Results discount the corner enhancement effect as the primary reason for the effective contribution of corners to contour integration. With every element in a stimulus a corner, no contour element is inherently singled out, yet all-corner contours retain high levels of visibility above 90% correct responses. The use of all-corner stimuli also dispels any concern about possible effects attributable to differences in spatial frequency spectra between corners and mono-oriented elements.

## Discussion

In a series of five experiments we investigated the role of corner elements in contour integration and determined geometric properties that characterize effective corners. We compared spatial and temporal dynamics of contour integration with and without corners in order to discern whether both may be predicated on a common neural process. We finally asserted that contour integration is functional for contours that contain nothing but corners. Put short, corners are highly effective in facilitating the integration of jagged contours, regardless of whether contours are constructed from narrowband or broadband stimulus elements.

Four important conclusions may be drawn from our observations. First, corners make contours with arbitrary inflection angles as salient as perfectly straight contours. Second, effective corners are not simply intersections ("+") but tip-to-tip collocations of two orientation components ("⊥"). Third, the contour completion mechanism can act solely on corners without intermediate mono-oriented elements. Finally, contour integration with corners is a spatially limited process unable to link corner elements across wider spatial distances.

Corner elements inform the observer about abrupt changes in path curvature. They allow for a reliable prediction of the further course as if the contour was perfectly straight. Corners thus help to constitute a particular form of good continuation (Metzger, 2006) where form completion no longer depends on the smoothness of global curvature but also incorporates local signals of orientation change. Although our results demonstrate highly similar characteristics for contour integration with and without corners, it is premature to conclude that both are invoking a single, shared mechanism. Equivalent psychophysical performance could be produced by both types of contour integration invoking the same neural mechanism, or by different mechanisms with similar dynamic properties.

The important role of nonlinear connectors such as corners for visual scene representation is a well-established fact and crucial to many fundamental theories of vision (Biederman, 1987; Marr, 1982). Although the neural architecture of corner detectors is far from definitive, studies agree that the processing of corners encompasses a hierarchy of neuron populations from different cortical layers (Hansen & Neumann, 2008). Multiple neuron populations in the ventral pathway from V1 to V4 and IT are involved in extracting complex object features like corners and crossings (Kobatake & Tanaka, 1994). Selectivity increases significantly towards V4 (Gallant, Connor, Rakshit, Lewis, & Van Essen, 1996), where corners are likely represented as locations of convexity and concavity at specific angles (Pasupathy & Connor, 2002).

Can the contribution of corners to contour integration be modeled as a simple extension of an association field model, presumably relocated to V4? Highly informative in this regard is the difference in contour integration performance with actual corner elements compared to mono-oriented elements and crossings.

Contour integration remained intact only with actual corner elements but fell to chance level when angular discontinuities were bridged by mono-oriented elements. With crossings, contour integration also deteriorated sharply for increasing angular discontinuity before stabilizing moderately above chance level at higher inflection angles. Corners in contour integration are demonstrably more than just the presence of two single orientation components in the same spatial location (Ito & Komatsu, 2004). Contour integration remains fully functional only with unambiguous corner signals, and for these signals dedicated corner detectors exist in area V4 (Pasupathy & Connor, 2002). This adds to the assumption of a link between corner detection and contour integration since recent studies have shown that contour integration is a backpropagating process, starting in area V4 and projecting down to multiple earlier cortical sites (Chen et al., 2014; Gilad et al., 2013). The extraction of contour information in V4 is thus deemed the cause rather than the outcome of contour related processing on earlier sensory sites (Shpaner, Molholm, Forde, & Foxe, 2013).

Our results suggest that association field theories of contour integration need to include mutual interconnections between neighboring orientation sensitive neurons of different complexity, ranging from simple orientation detectors to more complex units encoding corners with different preferred angles, and possibly other nonlinear connectors like crossings and junctions as well. This implies a geometric increase of cells and interconnections within one cortical layer. The existence of such a mechanism is corroborated by the fact that contour integration does not even require the presence of mono-oriented elements but is fully functional also for all-corner stimuli. This is remarkable since all-corner stimuli enforce that only two neighboring orientation components can ever be collinear along any given contour. Assemblies of two collinear but spatially disjoint orientation components do not qualify as contours and are not recognized as such by the visual system (Tversky, Geisler, & Perry, 2004). At the same time, our results reinforce the notion that contour integration is cardinally reliant on local orientation signals. When local orientation is eliminated from a contour stimulus, as with non-oriented blobs, or made ambiguous as with crossings, contour integration deteriorates or even ceases entirely.

Aside from focusing on collinear assemblies of local elements, it might be fruitful to posit contour integration as the result of a more complex cortical network for texture segmentation (Ben-Shahar & Zucker, 2004) that detects objects as well as object boundaries (Kourtzi & Kanwisher, 2001). Under advantageous viewing conditions, this network operates on contiguous object boundaries and effortlessly binds the output from neighboring detectors into complete percepts (Hansen & Neumann, 2008). In cluttered or ambiguous visual scenes, the system has the capacity to interpolate across space. It can exploit signals of collinearity, local curvature, and angular discontinuity to form a coherent percept of sparsely defined textures and texture boundaries (Landy & Bergen, 1991). Networks where corners, junctions and crossings are seamlessly integrated have been proposed to underlie several visual phenomena like curve detection (Link & Zucker, 1988; Takeichi, 1995; Zucker, Dobbins, & Iverson, 1989) and amodal contour completion (Kanizsa, 1976; Lerner, Hendler, & Malach, 2002; Williams & Jacobs, 1997), or illusory contour completion (Hirsch et al., 1995; Peterhans & von der Heydt, 1989; Westheimer & Li, 1997).

*Keywords: contour integration, corners, curvature, temporal dynamics, association field*

## Acknowledgments

## References

Alais, D., Blake, R., & Lee, S. H. (1998). Visual features that vary together over time group together over space. *Nature Neuroscience*, *1*(2), 160–164. Retrieved from http://www.ncbi.nlm.nih.gov/pubmed/10195133, doi:10.1038/414.

Angelucci, A., Levitt, J. B., Walton, E. J., Hupe, J. M., Bullier, J., & Lund, J. S. (2002). Circuits for local and global signal integration in primary visual cortex. *The Journal of Neuroscience: The Official Journal of the Society for Neuroscience*, *22*(19), 8633–8646. Retrieved from http://www.ncbi.nlm.nih.gov/pubmed/12351737

Anzai, A., Peng, X., & Van Essen, D. C. (2007). Neurons in monkey visual area V2 encode combinations of orientations. *Nature Neuroscience*, *10*(10), 1313–1321. Retrieved from http://www.ncbi.nlm.nih.gov/pubmed/17873872, doi:10.1038/nn1975.

Attneave, F. (1954). Some informational aspects of visual perception. *Psychological Review*, *61*(3), 183–193. Retrieved from https://pdfs.semanticscholar.org/6d01/98460198fdb49b89d1646049712b3a0683df.pdf

Ben-Shahar, O., & Zucker, S. W. (2004). Sensitivity to curvatures in orientation-based texture segmentation. *Vision Research*, *44*(3), 257–277. Retrieved from http://www.ncbi.nlm.nih.gov/pubmed/14642898

Bertamini, M., Helmy, M., & Bates, D. (2013). The visual system prioritizes locations near corners of surfaces (not just locations near a corner). *Attention, Perception & Psychophysics*, *75*(8), 1748–1760. Retrieved from https://www.ncbi.nlm.nih.gov/pubmed/25341647, doi:10.3758/s13414-013-0514-1.

Biederman, I. (1987). Recognition-by-components: A theory of human image understanding. *Psychological Review*, *94*(2), 115–145, doi:10.1037/0033-295x.94.2.115.

Bowden, V. K., Dickinson, J. E., Fox, A. M., & Badcock, D. R. (2015). Global shape processing: A behavioral and electrophysiological analysis of both contour and texture processing. *Journal of Vision*, *15*(13):18, 1–23, doi:10.1167/15.13.18. [PubMed] [Article]

Braun, J. (1999). On the detection of salient contours. *Spatial Vision*, *12*(2), 211–225, doi:10.1163/156856899x00120.

Burnham, B. R., & Neely, J. H. (2007). Involuntary capture of visual-spatial attention occurs for intersections, both real and "imagined". *Psychonomic Bulletin & Review*, *14*(4), 735–741. Retrieved from http://www.ncbi.nlm.nih.gov/pubmed/17972742

Chen, M. G., Yan, Y., Gong, X. J., Gilbert, C. D., Liang, H. L., & Li, W. (2014). Incremental integration of global contours through interplay between visual cortical areas. *Neuron*, *82*(3), 682–694. Retrieved from https://www.ncbi.nlm.nih.gov/pubmed/24811385, doi:10.1109/icdmw.2007.16.

Choe, Y., & Miikkulainen, R. (2004). Contour integration and segmentation with self-organized lateral connections. *Biological Cybernetics*, *90*(2), 75–88, doi:10.1007/s00422-003-0435-5.

Cole, G. G., Gellatly, A., & Blurton, A. (2001). Effect of object onset on the distribution of visual attention. *Journal of Experimental Psychology. Human Perception and Performance*, *27*(6), 1356–1368. Retrieved from http://www.ncbi.nlm.nih.gov/pubmed/11766930

Cole, G. G., Skarratt, P. A., & Gellatly, A. R. (2007). Object and spatial representations in the corner enhancement effect. *Perception & Psychophysics*, *69*(3), 400–412. Retrieved from http://www.ncbi.nlm.nih.gov/pubmed/17672428

Dakin, S. C., & Hess, R. F. (1999). Contour integration and scale combination processes in visual edge detection. *Spatial Vision*, *12*(3), 309–327, doi:10.1163/156856899x00184.

Ernst, U. A., Mandon, S., Schinkel-Bielefeld, N., Neitzel, S. D., Kreiter, A. K., & Pawelzik, K. R. (2012). Optimality of human contour integration. *PLoS Computational Biology*, *8*(5), e1002520. Retrieved from http://www.ncbi.nlm.nih.gov/pubmed/22654653, doi:10.1371/journal.pcbi.1002520.

Feldman, J., & Singh, M. (2005). Information along contours and object boundaries. *Psychological Review*, *112*(1), 243–252. Retrieved from http://www.ncbi.nlm.nih.gov/pubmed/15631595, doi:10.1037/0033-295X.112.1.243.

Field, D. J., Hayes, A., & Hess, R. F. (1993). Contour integration by the human visual system: Evidence for a local "association field". *Vision Research*, *33*(2), 173–193, doi:10.1016/0042-6989(93)90156-q.

Gallant, J. L., Connor, C. E., Rakshit, S., Lewis, J. W., & Van Essen, D. C. (1996). Neural responses to polar, hyperbolic, and Cartesian gratings in area V4 of the macaque monkey. *Journal of Neurophysiology*, *76*(4), 2718–2739. Retrieved from http://www.ncbi.nlm.nih.gov/pubmed/8899641

Geisler, W. S., Perry, J. S., Super, B. J., & Gallogly, D. P. (2001). Edge co-occurrence in natural images predicts contour grouping performance. *Vision Research*, *41*(6), 711–724, doi:10.1016/s0042-6989(00)00277-7.

Gilad, A., Meirovithz, E., & Slovin, H. (2013). Population responses to contour integration: Early encoding of discrete elements and late perceptual grouping. *Neuron*, *78*(2), 389–402. Retrieved from http://www.ncbi.nlm.nih.gov/pubmed/23622069, doi:10.1016/j.neuron.2013.02.013.

Grossberg, S., & Mingolla, E. (1985a). Neural dynamics of form perception: Boundary completion, illusory figures, and neon color spreading. *Psychological Review*, *92*(2), 173–211. Retrieved from http://www.cns.bu.edu/Profiles/Grossberg/GroMin1985PsychRev.pdf

Grossberg, S., & Mingolla, E. (1985b). Neural dynamics of perceptual grouping: Textures, boundaries, and emergent segmentations. *Perception & Psychophysics*, *38*(2), 141–171. Retrieved from https://link.springer.com/article/10.3758/BF03198851

Hansen, T., & Neumann, H. (2008). A recurrent model of contour integration in primary visual cortex. *Journal of Vision*, *8*(8):8, 1–25, doi:10.1167/8.8.8. [PubMed] [Article]

Heitger, F., Rosenthaler, L., von der Heydt, R., Peterhans, E., & Kubler, O. (1992). Simulation of

neural contour mechanisms: From simple to end-stopped cells. *Vision Research*, *32*(5), 963–981. Retrieved from http://www.ncbi.nlm.nih.gov/pubmed/1604865, doi:10.1016/0042-6989(92)90039-1.

Hess, R. F., & Dakin, S. C. (1997). Absence of contour linking in peripheral vision. *Nature*, *390*(6660), 602–604, doi:10.1038/37593.

Hess, R. F., & Field, D. (1999). Integration of contours: New insights. *Trends in Cognitive Sciences*, *3*(12), 480–486, doi:10.1016/s1364-6613(99)01410-2.

Hess, R. F., Hayes, A., & Kingdom, F. A. (1997). Integrating contours within and through depth. *Vision Research*, *37*(6), 691–696.

Hirsch, J., DeLaPaz, R. L., Relkin, N. R., Victor, J., Kim, K., Li, T., . . . Shapley, R. (1995). Illusory contours activate specific regions in human visual cortex: evidence from functional magnetic resonance imaging. *Proceedings of the National Academy of Sciences, USA*, *92*(14), 6469–6473. Retrieved from http://www.ncbi.nlm.nih.gov/pubmed/7604015

Ito, M., & Komatsu, H. (2004). Representation of angles embedded within contour stimuli in area V2 of macaque monkeys. *The Journal of Neuroscience: The Official Journal of the Society for Neuroscience*, *24*(13), 3313–3324. Retrieved from http://www.ncbi.nlm.nih.gov/pubmed/15056711, doi:10.1523/jneurosci.4364-03.2004.

Kanizsa, G. (1976). Subjective contours. *Scientific American*, *234*(4), 48–52. Retrieved from https://www.ncbi.nlm.nih.gov/pubmed/1257734.

Kinoshita, M., Gilbert, C. D., & Das, A. (2009). Optical imaging of contextual interactions in V1 of the behaving monkey. *Journal of Neurophysiology*, *102*(3), 1930–1944. Retrieved from http://www.ncbi.nlm.nih.gov/pubmed/19587316, doi:10.1152/jn.90882.2008.

Kobatake, E., & Tanaka, K. (1994). Neuronal selectivities to complex object features in the ventral visual pathway of the macaque cerebral cortex. *Journal of Neurophysiology*, *71*(3), 856–867. Retrieved from http://www.ncbi.nlm.nih.gov/pubmed/8201425

Kourtzi, Z., & Kanwisher, N. (2001). Representation of perceived object shape by the human lateral occipital complex. *Science*, *293*(5534), 1506–1509, doi:10.1126/science.1061133.

Landy, M. S., & Bergen, J. R. (1991). Texture segregation and orientation gradient. *Vision Research*, *31*(4), 679–691. Retrieved from http://www.ncbi.nlm.nih.gov/pubmed/1843770

Ledgeway, T., Hess, R. F., & Geisler, W. S. (2005). Grouping local orientation and direction signals to extract spatial contours: Empirical tests of "association field" models of contour integration. *Vision Research*, *45*(19), 2511–2522. Retrieved from http://www.ncbi.nlm.nih.gov/pubmed/15890381

Lerner, Y., Hendler, T., & Malach, R. (2002). Object-completion effects in the human lateral occipital complex. *Cerebral Cortex*, *12*(2), 163–177. Retrieved from http://www.ncbi.nlm.nih.gov/pubmed/11739264

Li, Z. (1998). A neural model of contour integration in the primary visual cortex. *Neural Computation*, *10*(4), 903–940.

Link, N. K., & Zucker, S. W. (1988). Corner detection in curvilinear dot grouping. *Biological Cybernetics*, *59*(4–5), 247–256. Retrieved from http://www.ncbi.nlm.nih.gov/pubmed/3196769

Mandon, S., & Kreiter, A. K. (2005). Rapid contour integration in macaque monkeys. *Vision Research*, *45*(3), 291–300.

Marr, D. (1980). Visual information processing: The structure and creation of visual representations. *Philosophical Transactions of the Royal Society of London. Series B, Biological Sciences*, *290*(1038), 199–218. Retrieved from http://www.ncbi.nlm.nih.gov/pubmed/6106238, doi:10.1007/978-3-642-93199-4_4.

Marr, D. (1982). *Vision: A computational investigation into the human representation and processing of visual information*. San Francisco, CA: Freeman.

Mathes, B., & Fahle, M. (2007). Closure facilitates contour integration. *Vision Research*, *47*(6), 818–827. Retrieved from http://www.ncbi.nlm.nih.gov/pubmed/17286999

Metzger, W. (2006). *Laws of seeing*. Cambridge, MA: MIT Press.

Mundhenk, T. N., & Itti, L. (2005). Computational modeling and exploration of contour integration for visual saliency. *Biological Cybernetics*, *93*(3), 188–212.

Parent, P., & Zucker, S. W. (1989). Trace inference, curvature consistency, and curve detection. *IEEE Transactions on Pattern Analysis and Machine Intelligence*, *11*(8), 823–839.

Pasupathy, A., & Connor, C. E. (2002). Population coding of shape in area V4. *Nature Neuroscience*, *5*(12), 1332–1338. Retrieved from http://www.ncbi.nlm.nih.gov/pubmed/12426571, doi:10.1038/nn972.

Peterhans, E., & von der Heydt, R. (1989). Mechanisms of contour perception in monkey visual cortex. II. Contours bridging gaps. *The Journal of Neurosci-*

ence: The Official Journal of the Society for Neuroscience, 9(5), 1749–1763. Retrieved from http://www.ncbi.nlm.nih.gov/pubmed/2723748

Pettet, M. W. (1999). Shape and contour detection. *Vision Research, 39*(3), 551–557. Retrieved from http://www.ncbi.nlm.nih.gov/pubmed/10341983

Poirier, F. J., & Wilson, H. R. (2007). Object perception and masking: Contributions of sides and convexities. *Vision Research, 47*(23), 3001–3011. Retrieved from http://www.ncbi.nlm.nih.gov/pubmed/17889924, doi:10.1016/j.visres.2007.08.003.

Rodrigues, J., & du Buf, J. M. (2006). Multi-scale keypoints in V1 and beyond: Object segregation, scale selection, saliency maps and face detection. *Biosystems, 86*(1–3), 75–90. Retrieved from http://www.ncbi.nlm.nih.gov/pubmed/16870327, doi:10.1016/j.biosystems.2006.02.019.

Roelfsema, P. R., Lamme, V. A., Spekreijse, H., & Bosch, H. (2002). Figure-ground segregation in a recurrent network architecture. *Journal of Cognitive Neuroscience, 14*(4), 525–537. Retrieved from http://www.ncbi.nlm.nih.gov/pubmed/12126495, doi:10.1162/08989290260045756.

Shevelev, I. A., Kamenkovich, V. M., & Sharaev, G. A. (2003). The role of lines and corners of geometric figures in recognition performance. *Acta Neurobiologiae Experimentalis, 63*(4), 361–368. Retrieved from http://www.ncbi.nlm.nih.gov/pubmed/15053259, doi:10.1016/s0306-4522(97)00393-x.

Shpaner, M., Molholm, S., Forde, E., & Foxe, J. J. (2013). Disambiguating the roles of area V1 and the lateral occipital complex (LOC) in contour integration. *Neuroimage, 69*, 146–156. Retrieved from http://www.ncbi.nlm.nih.gov/pubmed/23201366, doi:10.1016/j.neuroimage.2012.11.023.

Stettler, D. D., Das, A., Bennett, J., & Gilbert, C. D. (2002). Lateral connectivity and contextual interactions in macaque primary visual cortex. *Neuron, 36*(4), 739–750. Retrieved from http://www.ncbi.nlm.nih.gov/pubmed/12441061

Takeichi, H. (1995). The effect of curvature on visual interpolation. *Perception, 24*(9), 1011–1020. Retrieved from http://www.ncbi.nlm.nih.gov/pubmed/8552455, doi:10.1068/p241011.

Tversky, T., Geisler, W. S., & Perry, J. S. (2004). Contour grouping: Closure effects are explained by good continuation and proximity. *Vision Research, 44*(24), 2769–2777.

Ursino, M., & La Cara, G. E. (2004). A model of contextual interactions and contour detection in primary visual cortex. *Neural Networks: The Official Journal of the International Neural Network Society, 17*(5–6), 719–735. Retrieved from http://www.ncbi.nlm.nih.gov/entrez/query.fcgi?cmd=Retrieve&db=PubMed&dopt=Citation&list_uids=15288894

Vancleef, K., & Wagemans, J. (2013). Component processes in contour integration: A direct comparison between snakes and ladders in a detection and a shape discrimination task. *Vision Research, 92*, 39–46. Retrieved from http://www.ncbi.nlm.nih.gov/pubmed/24051198, doi:10.1016/j.visres.2013.09.003

Wagemans, J., Elder, J. H., Kubovy, M., Palmer, S. E., Peterson, M. A., Singh, M., & von der Heydt, R. (2012). A century of Gestalt psychology in visual perception: I. Perceptual grouping and figure-ground organization. *Psychological Bulletin, 138*(6), 1172–1217. Retrieved from http://www.ncbi.nlm.nih.gov/pubmed/22845751, doi:10.1037/a0029333.

Westheimer, G., & Li, W. (1997). Classifying illusory contours: Edges defined by "pacman" and monocular tokens. *Journal of Neurophysiology, 77*(2), 731–736. Retrieved from http://www.ncbi.nlm.nih.gov/pubmed/9065845

Williams, L. R., & Jacobs, D. W. (1997). Stochastic completion fields: A neural model of illusory contour shape and salience. *Neural Computation, 9*(4), 837–858. Retrieved from http://www.ncbi.nlm.nih.gov/pubmed/9161024

Williams, L. R., & Thornber, K. K. (2001). Orientation, scale, and discontinuity as emergent properties of illusory contour shape. *Neural Computation, 13*(8), 1683–1711. Retrieved from http://www.ncbi.nlm.nih.gov/pubmed/11506666, doi:10.1162/08997660152469305.

Yen, S. C., & Finkel, L. H. (1998). Extraction of perceptually salient contours by striate cortical networks. *Vision Research, 38*(5), 719–741.

Zucker, S. W., Dobbins, A., & Iverson, L. (1989). Two stages of curve detection suggest two styles of visual computation. *Neural Computation, 1*(1), 68–81, doi:10.1162/neco.1989.1.1.68